JOURNAL OF VIROLOGY, Feb. 2009, p. 1660–1668 Vol. 83, No. 4
0022-538X/09/$08.00+0 doi:10.1128/JVI.01139-08

Herpes Simplex Virus Replication: Roles of Viral Proteins and Nucleoporins in Capsid-Nucleus Attachment▽

Anna Maria Copeland, William W. Newcomb, and Jay C. Brown*

Department of Microbiology and Cancer Center, University of Virginia Health System, Charlottesville, Virginia 22908

Received 30 May 2008/Accepted 3 December 2008

Replication of herpes simplex virus type 1 (HSV-1) involves a step in which a parental capsid docks onto a host nuclear pore complex (NPC). The viral genome then translocates through the nuclear pore into the nucleoplasm, where it is transcribed and replicated to propagate infection. We investigated the roles of viral and cellular proteins in the process of capsid-nucleus attachment. Vero cells were preloaded with antibodies specific for proteins of interest and infected with HSV-1 containing a green fluorescent protein-labeled capsid, and capsids bound to the nuclear surface were quantified by fluorescence microscopy. Results showed that nuclear capsid attachment was attenuated by antibodies specific for the viral tegument protein VP1/2 (UL36 gene) but not by similar antibodies specific for UL37 (a tegument protein), the major capsid protein (VP5), or VP23 (a minor capsid protein). Similar studies with antibodies specific for nucleoporins demonstrated attenuation by antibodies specific for Nup358 but not Nup214. The role of nucleoporins was further investigated with the use of small interfering RNA (siRNA). Capsid attachment to the nucleus was attenuated in cells treated with siRNA specific for either Nup214 or Nup358 but not TPR. The results are interpreted to suggest that VP1/2 is involved in specific attachment to the NPC and/or in migration of capsids to the nuclear surface. Capsids are suggested to attach to the NPC by way of the complex of Nup358 and Nup214, with high-resolution immunofluorescence studies favoring binding to Nup358.

Herpes simplex virus type 1 (HSV-1) virions consist of four prominent structures: the viral membrane, the tegument, the DNA-containing capsid, and the DNA itself. The membrane is a host-derived lipid bilayer, typically spherical in shape, with the viral glycoproteins embedded in it. Among the glycoproteins are those that bind to host receptors and initiate fusion between the cell and viral membranes, releasing the DNA-containing capsid and tegument into the cytoplasm of the host cell.

Upon entry into the cytoplasm, the capsid is transported to the nucleus by way of its interactions with the minus-end-directed microtubule motor protein dynein (14, 43). During entry and transit to the nucleus, much of the tegument dissociates from the capsid (19, 32, 33, 43), although at least two tegument proteins, VP1/2 and UL37, remain associated (19, 32). Such partially tegumented capsids bind to the host nuclear pore complex (NPC), where the viral DNA is released, a process termed uncoating. The HSV-1 capsid remains on the cytoplasmic side of the NPC, while the DNA enters the nucleus by translocating through the pore (4, 27, 45).

NPCs are large multiprotein complexes that mediate transport into and out of the nucleus (2). The vertebrate nuclear pore is a 125-MDa complex (40) that traverses both the inner and outer nuclear membranes. Each pore is composed of more than 30 different proteins (11), called nucleoporins, that are arranged with eightfold symmetry (16). NPCs can be thought of in terms of three structural regions: the nuclear basket, the central core, and the cytoplasmic filaments. The basket resides inside the nucleus, the central core is in the plane of the nuclear envelope, and the cytoplasmic filaments project into the cytoplasm (15, 44). The filaments are composed primarily of Nup358 (12, 47, 50), with Nup214 and Nup88 existing as a complex on the cytoplasmic face of the NPC (3, 28, 39). By projecting into the cytoplasm, the filaments are in a position to interact with HSV-1 capsids.

Capsid binding to the NPC occurs with a distinctive orientation. The capsid binds with a vertex facing the pore channel at a characteristic distance (40 to 50 nm) above the pore (A.M.C., unpublished observations) (18, 38). This distance is consistent with a possible interaction with the 35- to 50-nm-long cytoplasmic filaments (5, 17, 30). Additionally, interactions have been observed between nucleus-bound HSV-1 capsids and filaments emanating from the nucleus (43).

Nuclear capsid binding and genome uncoating are two processes that have remained poorly understood. The cellular factors importin-β and Ran-GTP are essential for binding (38), but neither the nucleoporins nor the viral proteins involved have been identified. VP1/2 has recently been shown to play a role in uncoating, long implied by the *ts*B7 mutant (26). *ts*B7 HSV-1 has a defect that allows nuclear capsid binding but not uncoating at the nonpermissive temperature (4, 45). The mutation maps to UL36, the gene encoding VP1/2 (4). Following nuclear capsid binding, VP1/2 is cleaved to allow uncoating to proceed (26). VP1/2's role in nuclear binding and the possible involvement of other herpesvirus proteins are not well understood.

Here we describe the results of studies in which we tested the involvement of herpesvirus capsid and tegument proteins and nucleoporins in the early steps in infection. Blocking experiments were performed with the use of herpesvirus and nucleoporin antibodies introduced into cells by syringe load-

* Corresponding author. Mailing address: Department of Microbiology, Box 800734, University of Virginia Health System, 1300 Jefferson Park Ave., Charlottesville, VA 22908. Phone: (434) 924-2504. Fax: (434) 982-1071. E-mail: jcb2g@virginia.edu.

▽ Published ahead of print on 10 December 2008.

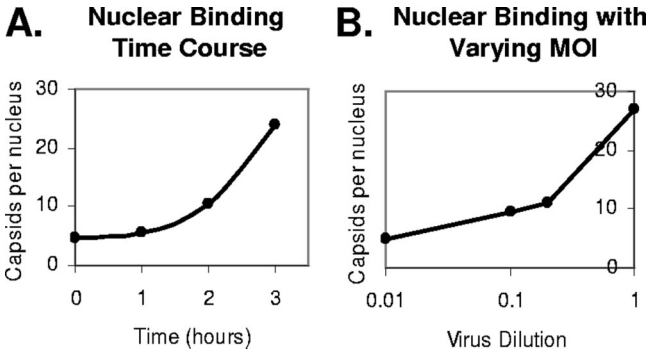

FIG. 1. Nuclear capsid quantification. (A) Graph of nuclear capsid binding over time. (B) Graph of nuclear capsid binding increase with increased MOI.

ing. Additionally, microscopy and small interfering RNA (siRNA) were used to address the involvement of nucleoporins. Specifically, Nup358 was our primary candidate because of its localization to the distal end of the cytoplasmic filaments (47). On the viral side, VP1/2 was of particular interest because of its role in uncoating, previous implications of VP1/2's involvement in nuclear binding, and its purported localization to the capsid vertices (8, 36, 38, 51).

Our results show that VP1/2 plays an important role early in infection prior to uncoating and that Nup358 is important for HSV-1 nuclear capsid binding.

MATERIALS AND METHODS

Cells, viruses, and virus concentration. All experiments were performed with Vero cells and with the K26GFP (13) strain of HSV-1 (a gift of Prashant Desai). K26GFP is a KOS-derived mutant in which the gene encoding UL35 is fused to the green fluorescent protein (GFP) gene. Capsids appear green when viewed by epifluorescence due to incorporation of GFP-tagged UL35 into capsids.

Vero cells were maintained in 150-cm^2 flasks at 37°C with 7.5% CO_2 in minimal essential medium (MEM) with 10% fetal bovine serum (FBS), L-glutamine, and antibiotics. For large-scale virus purification, Vero cells were passed to six 850-cm^2 polystyrene roller bottles. Prior to infection, cells were washed one time with 30 ml per roller bottle MEM with 1% FBS, L-glutamine, and antibiotics. HSV-1 K26GFP was added at a multiplicity of infection of 3 and allowed to attach for 1 h in a low medium volume (23 ml per bottle MEM, 1% FBS with L-glutamine and antibiotics). Medium volumes were then increased to 56 ml per bottle, and cells were incubated for 24 h at 37°C. Virus was then concentrated. For this, medium was collected and spun in a clinical centrifuge to pellet cells and cell debris. The pellets were discarded, and the supernatant was saved. The supernatant was centrifuged for 1 h at 23,000 rpm at 4°C in a Beckman SW28 rotor to produce virus-containing pellets. Pellets were resuspended in 1× phosphate-buffered saline (PBS), aliquoted, and frozen.

Syringe loading. This method was adapted from that of Clark and McNeil (7). Syringe loading is a method that allows the introduction of antibodies directly into the cytoplasm of cells by shearing the cell membrane in an antibody-rich solution. Small membrane tears allow the antibody to enter the cytoplasm. Tears then reseal, leaving a living cell with antibody in the cytoplasm. For syringe loading experiments, one 150-cm^2 flask of Vero cells (5×10^7 cells) was trypsinized. One-fourth of the cells were washed, suspended in 1.5 ml serum-free MEM, and allowed to rest for 20 min at 37°C with 7.5% CO_2. For each sample, 66 μl of the cell suspension was mixed with Pluronic-68 (Sigma-Aldrich) to a concentration of 2% (wt/vol) and antibody at a concentration between 0.2 and 1 mg/ml. The samples were taken up and down through a 27-gauge needle for a total of 50 strokes. The cells were then pelleted at 2,500 rpm for 5 min and resuspended in MEM (supplemented with L-glutamine and antibiotics) with 10% FBS. Cells were then plated in eight-well chambered cover glasses (growth area, 0.7 cm^2 per chamber) (Nunc* Lab-Tek* II chambered cover glasses).

Quantification of nuclear capsids. To assess nuclear capsid binding, multiple confocal images were taken of infected cells. Images were central nuclear sections. Each green dot present on the nuclear annulus was counted and scored as representing one capsid. To validate the method, a time course was quantified. At early time points (0 and 1 h postinfection), very few capsids were present on the nuclear surface (Fig. 1A). At 2 h postinfection, a moderate increase was observed, and a sharp increase in nuclear capsids was seen by 3 h postinfection (Fig. 1A). Additionally, various virus dilutions were tested in infection. In these experiments, green dots on the nuclear surface increased with increasing multiplicities of infection (MOIs) (Fig. 1B).

Microscopy and image processing. All fluorescence microscopy was done with a Nikon Eclipse TE2000-E fluorescence microscope (Improvision Open Lab software) or a Zeiss LSM 510 confocal microscope. Prior to grouping images, a calibration image was used to find the optimal contrast for each individual color. All experimental images were then adjusted to those calibration image settings. After images were compiled and grouped, the contrast was enhanced on two of the grouped figures using Adobe's Photoshop software.

siRNA. Vero cells were plated in 96-well plates (0.32-cm^2 growth area per well) in antibiotic-free MEM with 10% fetal calf serum at 60% confluence 24 h prior to transfection. A lipid transfection reagent was used to deliver targeted RNA duplexes and nontargeted control RNA duplexes at a final concentration of 100 nm. More specifically, pools of targeted double-stranded RNA duplexes were obtained from Dharmacon (ON-TARGETplus SMARTpools). Four sequence targets were used per gene (Nup358 sense sequences, GCGAAGUGA UGAUAUGUUU, CAAACCACGUUAUUACUAA, CAGAACAACUUGC UAUUAG, and GAAGGAAUGUUCAUCAGGA; TPR sense sequences, GA AGAAGUGCGUAAGAAUA, UCAGUUGACUCCAGGAAUA, UCAAGG AGGUUUAGGAAUG, and GGCAUACACUUACUAGAAA; and Nup214 sense sequences, UCAAAUACCUCUAACCUAU, GCAACACCCUCCACUA AAG, GAAAUCGUGACUCUGGUUA, and CCACAAGCCUAACUAGU AC). Sequence targets were derived from human sequences because of a lack of green monkey (Vero cell) sequence availability. Each duplex pool was diluted to 10 μM in 1× buffer (10 mM KCl, 6 mM HEPES [pH 7.5], 0.2 mM $MgCl_2$). DharmaFECT lipid reagent 1 was diluted 1:8 in serum-free, antibiotic-free MEM. siRNAs were further diluted in serum-free, antibiotic-free MEM (7.4 μl 10 μM siRNA with 105 μl MEM). This siRNA solution was incubated for 30 min at room temperature with lipid and serum-free MEM (100 μl siRNA, 10 μl lipid, 90 μl MEM). After incubation, 450 μl MEM with 10% fetal calf serum was added to each sample. One hundred microliters of this 100 nM solution was added per well and allowed to incubate at 37°C with 7.5% CO_2 for 24 h. After 24 h, transfections were repeated. Forty-eight hours post-initial transfection, cells were trypsinized and replated into eight-well chambered cover glasses to a confluence of 60%. At 72 h post-initial transfection, cells were infected with the K26GFP strain of HSV-1 at an MOI of 300. For infection, cells were brought to room temperature. Concentrated virus was added and allowed to attach for 1 h at 4°C in MEM with 1% fetal calf serum. The medium was then aspirated to remove any unattached virus. The medium was replaced with warm MEM with 1% fetal calf serum, and cells were incubated at 37°C with 7.5% CO_2 for 3 h. Cells were then washed one time with 1× PBS and fixed by submersion in 4% paraformaldehyde for 5 min. Cells were then washed three times with 1× PBS before being immunostained (described below) and viewed in the fluorescence microscope.

Immunofluorescence. Postfixation, cells were permeabilized by one of two methods: (i) submersion in ice-cold methanol for 4 min or (ii) submersion in digitonin (40 μg/ml in PBS) for 10 min at room temperature. Methanol-permeabilized cells were then washed once in 1× PBS, and digitonin-permeabilized cells were washed three times in 1× PBS, followed by blocking with 5% goat serum in 1× PBS at room temperature for 1 h. Primary antibody was added at the optimized dilution for 1 h at room temperature. Cells were washed three times in 1× PBS. Secondary antibodies (Alexa-conjugated goat antimouse or goat antirabbit [Molecular Probes]) were added at a dilution of 1:2,000 for 1 h at room temperature. Cells were washed three times in 1× PBS, and a 4′,6′-diamidino-2-phenylindole stain (0.5 μg/ml in 150 mM Tris-Cl [pH 7.5]) was added for 5 min. Cells were washed three times in 1× PBS and viewed by fluorescence microscopy.

Native labeling. Cells were grown in eight-well chambered cover glasses to 75% confluence. Cells were washed one time in 1× PBS and permeabilized by the addition of digitonin (40 μg/ml in PBS) for 10 min at room temperature. Cells were washed three times in 1× PBS and labeled as described above. After a final wash following secondary antibody removal, cells were fixed by submersion in 4% paraformaldehyde for 5 min.

Colocalization analysis. Confocal images were opened in the ImageJ software program (National Institutes of Health) and run through the Colocalization Finder plugin (C. Laummonerie and J. Metterer, 2006) to generate images in which colocalized pixels appear white. Images were then opened in Adobe

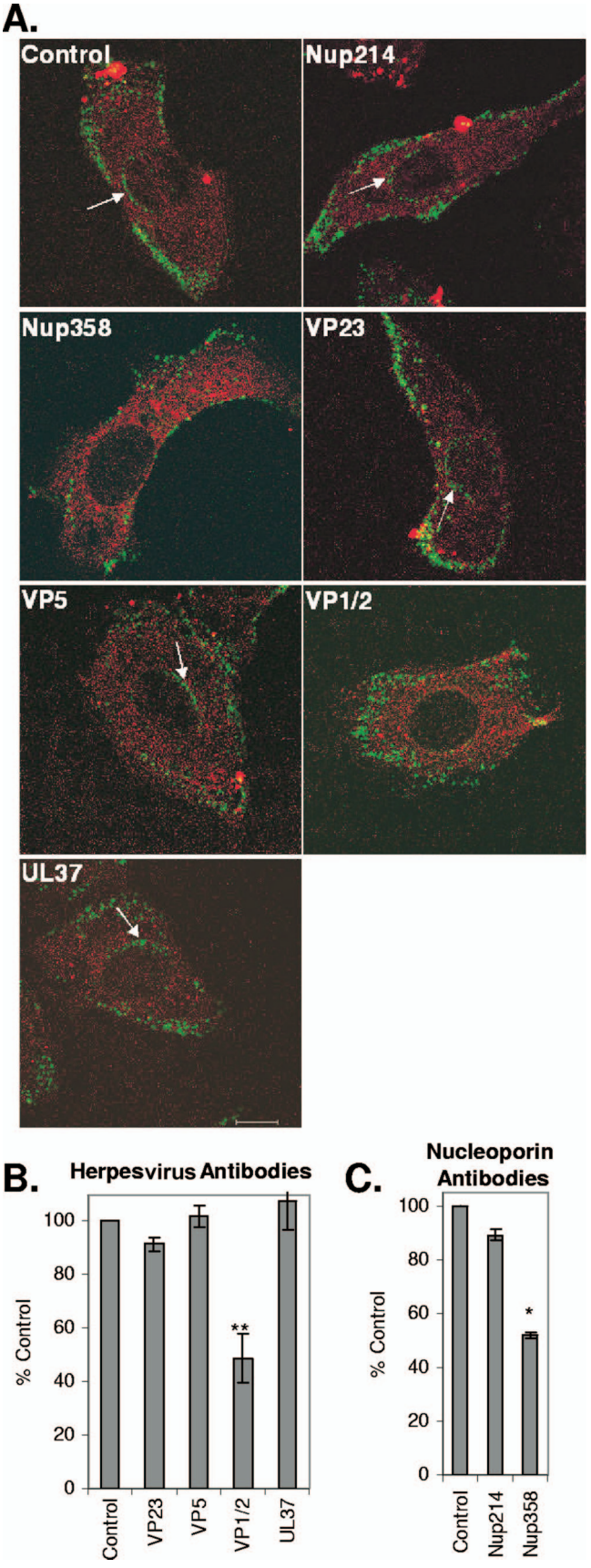

Photoshop. The numbers of white pixels and green pixels present on the nuclear surface were determined. The number of white pixels for each nucleus was divided by the total white and green pixels for the nucleus and expressed as a percentage. A total of 50 nuclei per sample were analyzed.

Antibodies. Anti-CD3 antibody was used as a control in syringe loading experiments. Anti-CD3 was purified from the hybridoma cell line CRL-1975 (29) (provided by Timothy P. Bender) and conjugated to Alexa-594 succinimidyl ester (Molecular Probes) to produce a control antibody that emits red fluorescence. The labeling instructions provided with the amine-reactive probe were followed. For Western blots, importin-β was used as a loading control and probed with monoclonal anti-importin-β (31H4; Sigma-Aldrich). For syringe loading experiments and immunofluorescence experiments, the following antibodies were used: anti-VP5 (6F) (34), anti-VP23 (1D2) (37), UL37 rabbit antiserum (42) (provided by Frank Jenkins), VP1/2 rabbit antiserum (48) (Schipke & Sodeik, personal communication) (provided by Beate Sodeik and Ari Helenius), Nup358 rabbit antiserum (49) (provided by Elias Coutavas and Günter Blobel), and Nup214 QE5 (39) (provided by Bryce Paschal). For syringe loading, monoclonal antibodies were used at a concentration of 1 mg/ml and serum was used undiluted, with the exception of Nup358 serum, which was diluted 1:100. For immunofluorescence, antibodies were used at the following dilutions: VP5, 1:250; VP23, 1:500; VP1/2, 1:250; UL37, 1:300; Nup358, 1:250; Nup214, 1:250; and TPR (1A8, Novus Biologicals), 1:600. For Western blots, antibodies were used at the following dilutions: Nup358, 1:1,000; Nup214, 1:500; TPR, 1:1,250; importin-β, 1:4,000.

RESULTS

Antibodies specific for VP1/2 and Nup358 reduce HSV-1 nuclear capsid binding. To test the involvement of specific herpesvirus proteins and nucleoporins in the process of capsid-nucleus attachment, antibodies specific for selected proteins were introduced directly into the cytoplasm of cells by syringe loading (see Methods). The cells were subsequently infected with HSV-1, and nuclear binding was assessed to determine if the presence of antibodies affected the capsid's ability to interact with the host nuclear pore. It was reasoned that antibodies would physically block capsid-nucleus interactions if they were bound to sites (either on NPCs or capsids) important for nuclear binding. We introduced herpesvirus-specific antibodies, control antibodies, and nucleoporin-specific antibodies to test the ability of each to perturb capsid-nucleus attachment. Antibody uptake was confirmed by coloading with an Alexa 594-conjugated control antibody. Cells that exhibited a red fluorescence signal in their cytoplasm were considered effectively loaded (Fig. 2A). Antibodies were introduced 3 to 4 h prior to infection with K26GFP HSV-1. After infection for 3 h, nuclear capsid binding was assessed by fluorescence microscopy and counts of capsids bound to the surface of the nucleus (visualized as green punctum present on the nuclear surface)

FIG. 2. Inhibition of nuclear capsid binding in syringe-loaded Vero cells. (A) Fluorescence micrographs of syringe-loaded Vero cells infected with HSV-1 K26GFP. Note that accumulations of capsids are present at the nuclear surface of cells loaded with the following antibodies: control, VP23, VP5, UL37, and Nup214 (arrows). (B) Graph showing the number of nucleus-bound capsids as a percentage of control in cells syringe-loaded with herpesvirus antibodies (anti-VP5, anti-VP23, anti-VP1/2, and anti-UL37). (C) Graph of nuclear capsid binding inhibition in cells loaded with nucleoporin antibodies (anti-Nup358 and anti-Nup214). In panels B and C, bars represent means of duplicate or triplicate (VP1/2 and Nup358) experiments with the standard error shown (*, $P = 0.0041$; **, $P < 0.0001$). An average of between 40 and 50 cells were analyzed per sample per experiment. Cells were infected 3 to 4 h after antibody loading. Nuclear binding was assessed 3 h postinfection.

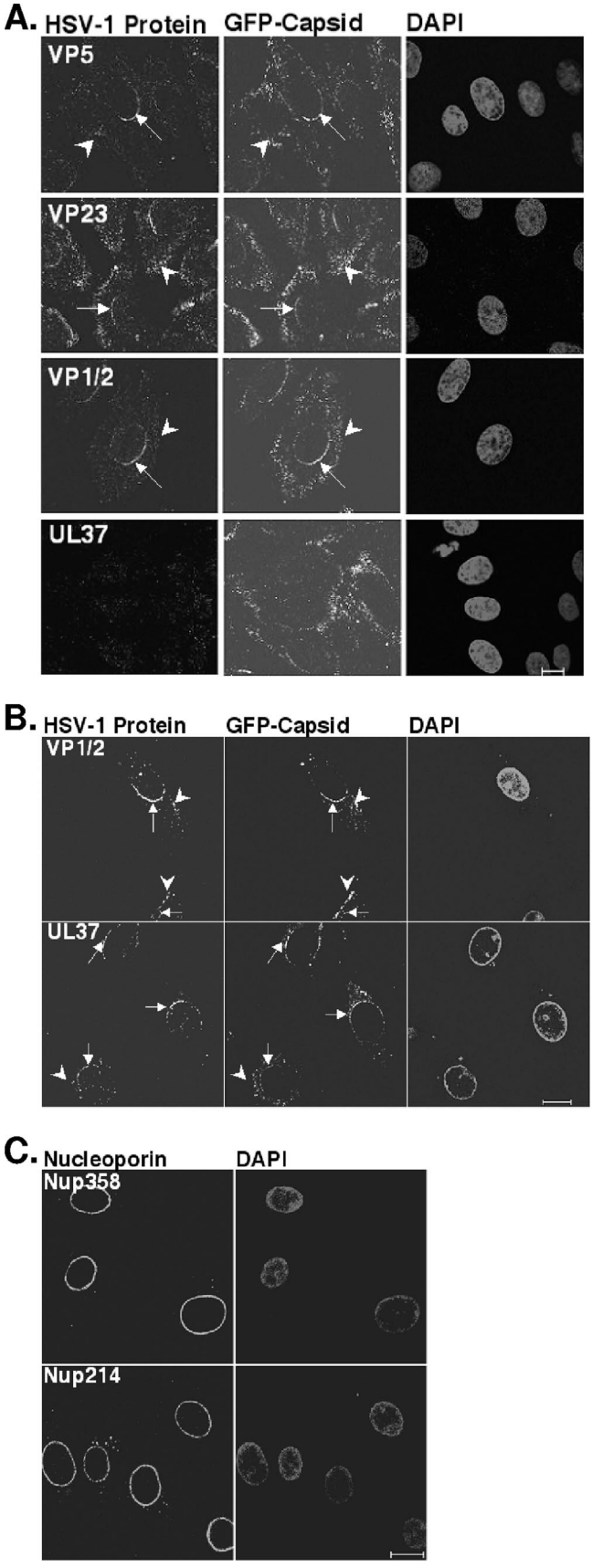

(Fig. 2A). A reduction in the number of nuclear capsids was interpreted as antibody interference with the capsid's ability to interact with the nuclear pore, indicating a role for the protein in the binding process.

The results show a binding reduction with anti-VP1/2, one of four herpesvirus antibodies tested (Fig. 2A and B). The presence of antibodies to VP5, the triplex component VP23, and UL37 in the cytoplasm of infected cells did not affect the ability of capsids to accumulate at the nuclear surface (Fig. 2A and B). The presence of antibodies to VP1/2 in the cytoplasm of infected cells led to a 51% reduction in nuclear capsid binding compared to results for controls (Fig. 2B). The ability of VP1/2 antibodies to reduce nuclear capsid binding is interpreted as evidence that VP1/2 is involved early in infection.

Since herpesvirus capsids bind on the cytoplasmic side of the nuclear pore, similar experiments were performed with antibodies specific for the cytoplasmic nucleoporins. Like capsid antibodies, nucleoporin-specific antibodies were introduced into the cytoplasm of cells prior to infection with the K26GFP strain of HSV-1. The presence of antibodies to the cytoplasmic filament protein Nup358 in the cytoplasm of infected cells coincided with a 48% reduction in nuclear capsid binding (Fig. 2A and C). A reduction was not seen with antibodies specific for the protein Nup214 (Fig. 2A and C). This result supports our hypothesis that capsids interact with the nuclear pore by way of the cytoplasmic filaments, specifically the filament protein Nup358.

Herpesvirus antibodies recognize target antigens in infected cells. To verify that herpesvirus antibodies were capable of binding to their target antigen in the context of intact capsids, immunofluorescence experiments were performed on cells infected with K26GFP HSV-1. In the case of VP5, VP23, and VP1/2, the antibody signal was coincident with the GFP capsid signal (Fig. 3A) in fixed cells. In unfixed cells, VP1/2 and UL37 showed staining coincident with the GFP capsid signal (Fig. 3B). Costaining was observed with virions at the cell surface and also with capsids at the nuclear surface (Fig. 3A and B). In unfixed cells, background levels were too high to allow analysis in cells stained with VP5 and VP23 antibody. The coincidence of the two fluorescent signals indicates that all four antibodies recognize capsid-associated antigen.

Native labeling with nucleoporin antibodies. Native labeling experiments were performed to verify that nucleoporin antibodies bound to their target antigen under conditions similar to those in syringe-loaded cells. For both Nup358 and Nup214, the antibody was introduced into the cytoplasm of unfixed

FIG. 3. Immunofluorescent labeling of herpesvirus proteins and nucleoporins. (A and B) Fluorescence micrographs of cells infected with K26GFP and immunolabeled for VP5, VP23, VP1/2, and UL37. Vero cells were infected with HSV-1 for 3 h, immunolabeled with antibodies against HSV-1 proteins, and visualized with Alexa 594-conjugated secondary antibodies. Capsids were detected by GFP signal. Note that GFP and protein labels occur coincidently at the cell surface (arrowheads) and at the nuclear surface (arrows) for VP5, VP23, VP1/2, and UL37. Scale bar, 10 μm. Cells in panel A were fixed prior to labeling, while cells in panel B were fixed after labeling. DAPI, 4′,6′-diamidino-2-phenylindole. (C) Unfixed cells were immunolabeled with nucleoporin antibodies. Both Nup358 and Nup214 antibodies exhibited a nuclear staining pattern consistent with interaction with their target antigen. Scale bar, 10 μm.

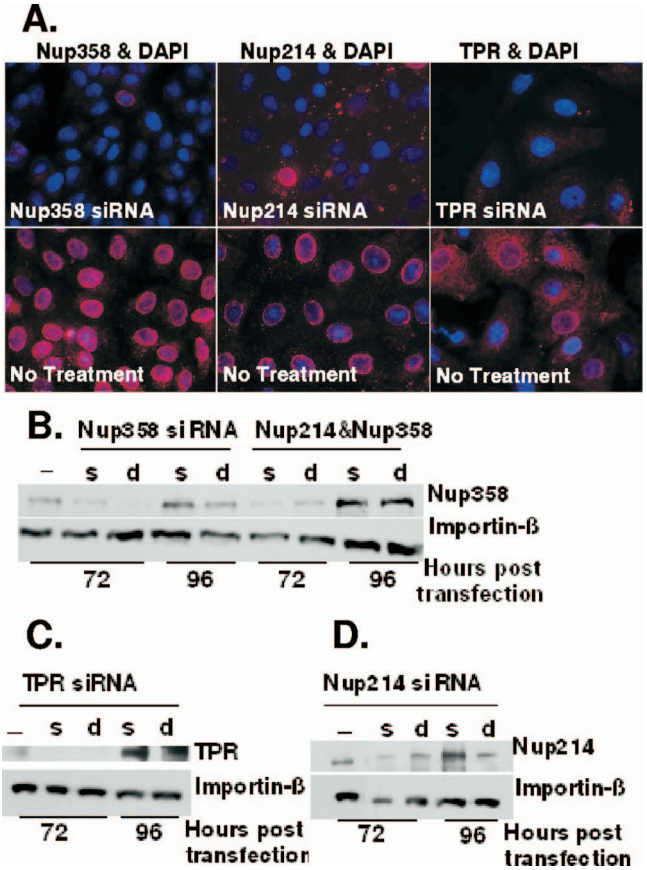

FIG. 4. Nucleoporin removal by siRNA treatment. (A) Fluorescence micrographs of immunolabeled Vero cells transfected with siRNAs specific for one of three nucleoporins: cytoplasmic filament protein Nup358, cytoplasmic facing protein Nup214, or nuclear basket protein TPR. Panels show nucleoporin signal (red) in siRNA-treated cells relative to signal in untreated cells. Treatment is indicated in the bottom left corner of each image, and staining is indicated at the top of each image column. (B to D) Western blots with importin-β serving as a loading control. Samples were taken 72 and 96 h posttransfection. "s" indicates cells transfected once. "d" indicates cells transfected twice, at 0 and 24 h post-initial transfection. (B) Western blot of Vero cells transfected with Nup358 siRNA alone and Nup358 siRNA plus Nup214 siRNA. (C) Western blot of Vero cells transfected with TPR siRNA. (D) Western blot of Vero cells transfected with Nup214 siRNA.

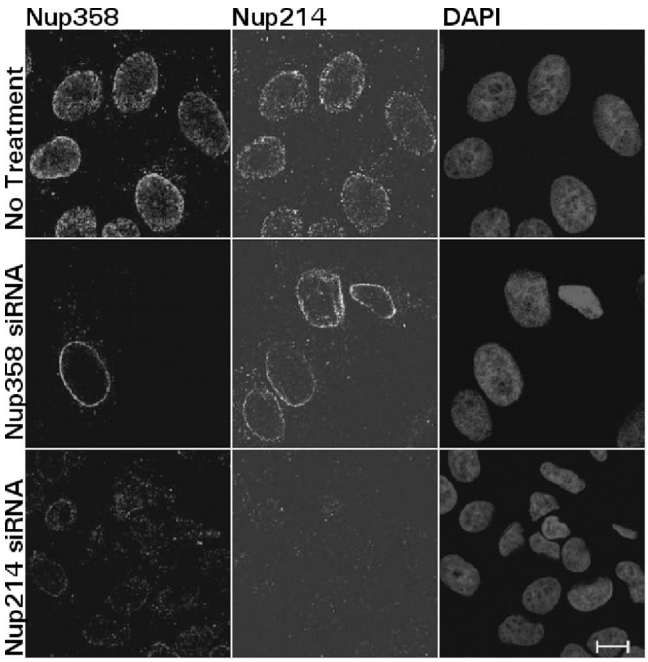

FIG. 5. Nup214 and Nup358 localization in siRNA-treated Vero cells. Fluorescence micrographs show nuclear localization patterns of Nup214 and Nup358 with three different treatments. Vero cells were transfected with siRNA specific for Nup214 or Nup358 or were given no treatment. Seventy-two hours after transfection, cells were fixed and immunostained for Nup214 and Nup358. Treatment is indicated to the left of the image row. Label is indicated at the top of the column of images. Note that untreated cells exhibit nuclear staining for both Nup358 and Nup214. Nuclear Nup358 and Nup214 staining are greatly reduced in Nup214 siRNA-treated cells. Nuclear Nup358 but not Nup214 is reduced in cells treated with Nup358 siRNA. DAPI, 4′,6′-diamidino-2-phenylindole. Scale bar, 10 μm.

cells. For each antibody, the resulting stain was seen exclusively at the nuclear surface (Fig. 3C). This is consistent with the expected staining pattern and thus indicates that Nup358 and Nup214 antibodies bind native antigen when introduced into the cytoplasm of cells.

Specific depletion of Nup358, Nup214, and TPR by siRNA. To further investigate the roles of nucleoporins in capsid-nucleus attachment, siRNAs were used to selectively remove nucleoporins from cells. Three nucleoporins were removed: TPR, Nup214, and Nup358. As a nuclear basket protein, TPR is not physically present on the cytoplasmic side of the nuclear pore, where herpesvirus capsids bind; therefore, its removal was not expected to influence nuclear capsid binding (9, 23). Protein reduction was assessed by Western blotting and immunofluorescence (Fig. 4). The greatest decreases in protein levels were observed at 72 h posttransfection (Fig. 4B to D), so this time was adopted for further experiments. Due to conflicting reports in the literature concerning the effect of silencing of Nup214 on the nuclear localization of Nup358 (6, 25), we performed double immunofluorescence labeling experiments to determine the effect of removal of Nup214 on Nup358 localization in our system.

We found that in cells treated with Nup214 siRNAs, removal of Nup214 resulted in a concurrent loss of Nup358 from the nuclear surface (Fig. 5) but not from the cell. With Nup214 siRNA treatment, cells maintained normal levels of Nup358 (Fig. 6B) as determined by Western blotting (data not shown), but localization to the nuclear surface was reduced. Nuclear loss of Nup358 was not observed in cells treated with either nonspecific control siRNAs or TPR siRNAs (data not shown). Treatment of cells with Nup358 siRNAs did not appear to reduce Nup214 nuclear localization (Fig. 5). These observations were consistent with a previous report that Nup214 plays a role in anchoring Nup358 to the nuclear surface (6); however, there exists some debate about this interaction (25, 47) (see the review in reference 31 for a discussion of relevant literature). We therefore cannot dismiss the possibility that off-target effects from Nup214 siRNA treatments are responsible for the Nup358 mislocalization.

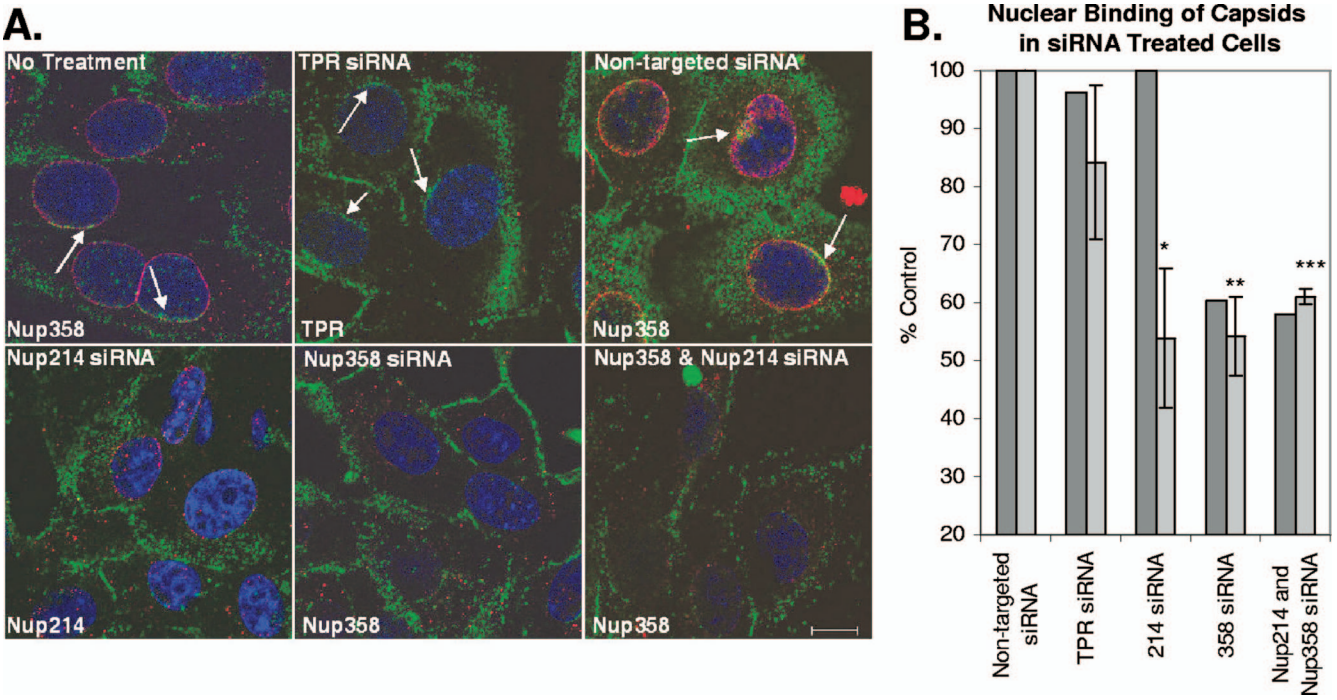

FIG. 6. Nuclear capsid binding in siRNA-treated cells. (A) Fluorescence micrographs of immunolabeled and 4′,6′-diamidino-2-phenylindole-stained siRNA-treated Vero cells infected with HSV-1 K26GFP. The siRNA treatment is indicated in the top left corner of each image. The cellular protein stained red is indicated in the bottom left. Capsids appear green. White arrows indicate accumulations of capsids at the nuclear surface 3 h postinfection. Scale bar, 10 μm. (B) Graph of Nup358 protein concentration (dark gray) and nuclear capsid binding (light gray) with standard error shown (*, $P = 0.0025$; **, $P < 0.0001$; **, $P = 0.002$). Note that nuclear capsid binding reduction corresponds to Nup358 protein concentration reduction except in the case of Nup214 siRNA, in which capsid binding is reduced in the absence of Nup358 protein reduction.

Nuclear capsid binding is reduced in cells depleted of Nup358 or Nup214. We infected siRNA-transfected cells 72 h after transfection, the time point of maximum protein reduction. As in syringe loading experiments, nuclear capsid binding was assessed by counts of GFP-labeled capsids present on the nuclear surface. Images of infected cells showed that untreated cells or cells treated with nontargeted siRNA or control TPR siRNA had accumulations of GFP-labeled capsids at the nuclear surface (Fig. 6A). Such accumulations were less often observed in cells treated with Nup358 siRNA, Nup214 siRNA, or both Nup358 and Nup214 siRNA (Fig. 6A). Counts from confocal images are summarized in Fig. 6B. The results showed that removal of the nuclear basket protein TPR failed to reduce the nuclear binding of capsids (Fig. 6B). In contrast, removal of Nup214, Nup358, or both Nup214 and Nup358 reduced nuclear capsid binding to 54%, 54%, and 61% of binding in control samples, respectively (Fig. 6B). For Nup358 siRNA-treated cells, nuclear capsid reduction corresponded to Nup358 protein concentration reductions to 60% of the control level (Fig. 6B). Our results suggest Nup358 is an important cellular factor involved in anchoring herpesvirus capsids to host nuclei. While Nup358 appears to be essential, these results are less revealing about Nup214's role in the binding process, since its removal could not be uncoupled from the removal of Nup358.

Nup358 resides exterior to Nup214 on the nuclear pore and colocalizes with HSV-1 capsids. To better understand the relative locations of Nup358, Nup214, and herpesvirus capsids, immunolabeled cells were examined by fluorescence microscopy. Immunogold studies have previously shown that Nup358 resides exterior to Nup214 on the nuclear pore (47). In light of this, single Nup214 and Nup358 stains were performed on cells infected with K26GFP HSV-1 to see if a difference could be observed in the degree of colocalization between GFP HSV-1 capsids and either Nup214 or Nup358. Capsids were found to colocalize with Nup358 (Fig. 7A, panels b and d) and to a lesser degree with Nup214 staining (Fig. 7A, panels a and c). The degree of colocalization was quantified and is expressed here as the percentage of the nuclear GFP capsid signal that overlapped with the red nucleoporin stain (Fig. 7B). The above results support the idea that the capsid attaches to Nup358.

DISCUSSION

Virus replication can begin only after the viral genome has been delivered to a site capable of supporting the production of viral gene products and replication of the viral genome. In the case of most DNA viruses, that means delivery of the viral DNA into the host cell nucleus. This presents DNA viruses with an interesting set of problems. The virus must sequester the genome from the cellular environment with a protective protein coat or capsid during trafficking to the nucleus while retaining the ability to release the genome from its protective location only at the appropriate time to allow uptake into the nucleus. The signals and mechanisms viruses use to coordinate these essential steps are not well understood.

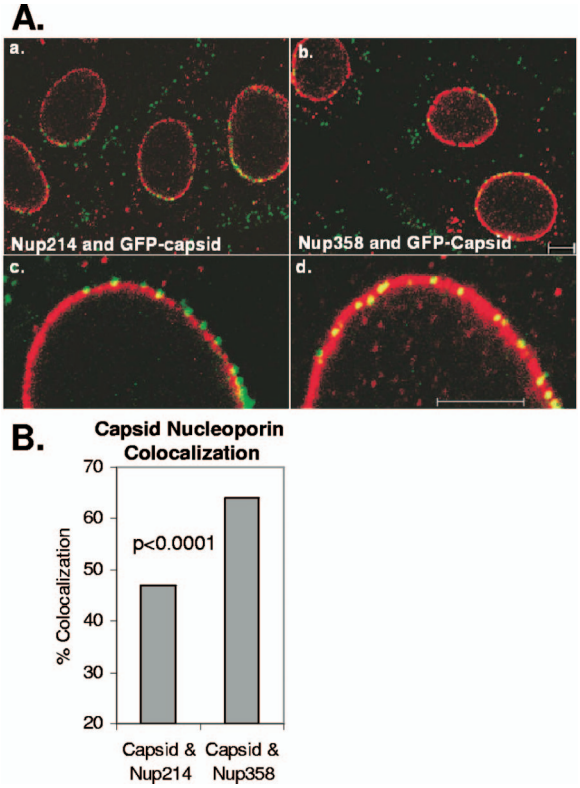

FIG. 7. Colocalization of herpesvirus capsids with Nup358 and Nup214. (A) Immunofluorescence of HSV-1 K26GFP-infected Vero cells. Cells were infected for 3 h and then fixed and stained for nucleoporins (red Nup214 in panels a and c or red Nup358 in panels b and d). High magnification of nuclear capsids is shown in panels c and d. A greater degree of colocalization was seen between capsids and Nup358 (panels b and d) than between capsid and Nup214 (panels a and c). Scale bar, 5 μm (panels a to d). (B) Graph of percent colocalization between capsids and nucleoporins. Each bar represents the number of green nuclear pixels overlapping with red nuclear pixels divided by the total number of green nuclear pixels, expressed as a percentage.

Some viruses employ a stepwise disassembly of the protective layers, initiated upon entry into the cell and completed at the host nucleus. Adenoviruses use this strategy. First, the fiber protein is removed when the virus is internalized. As the partially uncoated capsid is released from the endosome, a viral protease is activated, leading to further disassembly (10, 21, 22). Upon reaching the nuclear pore, the capsid interacts with Nup214, anchoring it to the pore (46). It is hypothesized that a loss of capsid integrity precedes DNA release. Following a loss of capsid integrity, the DNA translocates through the NPC as a complex with viral proteins (20, 41).

Herpesvirus virions also employ a stepwise disassembly; however, unlike the case with adenoviruses, herpesvirus capsids remain intact through the process. The viral envelope is removed from the capsid when it fuses with the cell membrane during entry. Much of the tegument also dissociates from the capsid upon entry and during transit to the nucleus (18, 19, 32, 33, 43). We have described tegument that is released from the capsid as loosely associated tegument and tegument that remains capsid bound (VP1/2 and UL37) as tightly associated (Fig. 8). Upon reaching the nucleus, HSV-1 capsids become anchored to the NPC. Nucleus-bound capsids have the interesting quality of being bound above the NPC with a vertex facing the pore. Our studies support the hypothesis that capsids attach to the NPC by way of an interaction with Nup358. Once bound to the NPC, a protease of unknown origin cleaves the tightly associated tegument, inducing a change that releases the viral DNA (26). HSV-1 genome uncoating resembles uncoating exhibited by double-stranded DNA bacteriophage, with the genome being extruded through the opening of a channel at a unique portal-containing vertex (35).

Here we sought to develop a system that would allow us to identify viral and cellular proteins involved in nuclear capsid binding in the context of a live infection. In syringe loading experiments, the presence of antibodies to VP1/2 but not other herpesvirus proteins in the cytoplasm of infected cells led to a decrease in the number of capsids bound to the nuclear surface

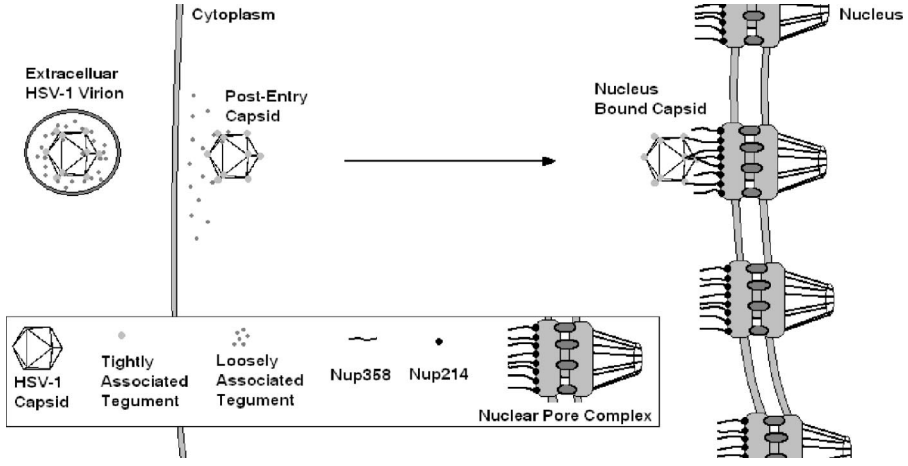

FIG. 8. Model of capsid binding at the nucleus. The model depicts the fate of HSV-1 capsids in newly infected cells. After fusion at the plasma membrane, the capsid and tegument enter the cytoplasm. Upon entry, loosely associated tegument is separated from the capsid, while a subset of tightly associated tegument proteins (VP1/2, UL37) remain attached as the capsid transits to the nucleus. Once at the nucleus, a vertex resident protein, possibly VP1/2, interacts with the pore to anchor the capsid with its distinctive vertex-to-pore orientation. Two nuclear pore proteins are highlighted in this model: Nup358 and Nup214. Herpesvirus capsids are shown bound to Nup358, the putative cytoplasmic filament protein.

(Fig. 2B). The ability of VP1/2 antibodies to reduce nuclear capsid binding is interpreted as evidence that VP1/2 is involved early in infection.

This experiment was designed to test the involvement of herpesvirus proteins in capsid nucleus attachment. However, two nonexclusive hypotheses could explain our results. VP1/2 antibodies may reduce nuclear capsid binding by attaching to capsids, physically interfering with the capsids' ability to interact with the nucleus, or VP1/2 antibodies may attach to capsids and impair the capsids' ability to travel to the nucleus, perhaps by perturbing the capsids' interaction with microtubule motor proteins.

Both interpretations are consistent with the observation that VP1/2 remains capsid associated in transit to the nucleus (19, 32). VP1/2 likely resides at the capsid vertices. Its location on the capsid depends on its interaction with the minor capsid protein UL25, which is found at the capsid vertices (8, 36, 51). A role for VP1/2 in nuclear binding could therefore explain the capsid's ability to orient itself at the nuclear pore with a vertex facing the center of the pore (18, 38).

Previous studies with HSV-1 provide further support for the hypothesis that VP1/2 is involved in contacting nuclear pores. Ojala and colleagues showed that proteolytic digestion of tegumented capsids reduced nuclear capsid binding in vitro. In the experiment, the following tegument proteins were digested: VP1/2, VP13/14, VP16, and VP22 (38). VP1/2 is likely the only one of the digested tegument proteins present on incoming capsids that reach the NPC.

Alternatively, VP1/2 may function in transporting capsids to the nucleus. This interpretation would be consistent with in vitro studies with HSV-1 showing that inner tegument proteins promote motility along microtubules (48).

Experiments were also done to investigate the involvement of nucleoporins in capsid-nucleus attachment. In syringe loading experiments, Nup358 antibodies alone were found to reduce nuclear capsid binding (Fig. 2C). The inhibition of nuclear binding upon addition of Nup358 antibodies indicates that Nup358 may play an important role in anchoring herpesvirus capsids to nuclei. The capsids' distance from the pore when bound (40 to 50 nm) (18, 38) is consistent with an interaction with Nup358, which extends out from the pore as eight filaments (35 to 50 nm in length) (5, 17, 30). Additionally, fluorescence microscopy studies showed that fluorescently labeled capsids colocalize with Nup358 to a greater degree than with Nup214 (Fig. 7). Nup358's role as the nuclear receptor for herpesvirus capsids was further supported by the reduction in nuclear binding seen when Nup358 was removed by siRNA treatment of cells (Fig. 6A and B).

In light of published literature (6), it was not entirely surprising that nuclear binding was also reduced in cells treated with Nup214 siRNA (Fig. 6A and B). Nup214's localization to the cytoplasmic entrance of the NPC channel and not to the cytoplasmic filaments (47) makes it improbable that Nup214 plays a direct role in capsid-nucleus attachment. Rather, the reduction of nuclear capsid binding in cells treated with Nup214 siRNA is more likely a result of the loss of nuclear Nup358 in these cells (confirmed by fluorescence microscopy [Fig. 5]).

Binding of herpesvirus capsids to host nuclei is a required step in herpesvirus infections. It is the first step in the complex and poorly understood process of genome uncoating. Our results support a model (Fig. 8) in which capsids attach to the nuclear surface by way of an interaction with Nup358. The previous report citing the involvement of importin-β in nuclear capsid binding points to an interaction between capsids and Nup358 that may be indirect (38). It is tempting to imagine that herpesviruses hijack the importin-β nuclear import pathway for delivery of genome-containing capsids to the nucleus. It was recently demonstrated that the large tegument protein VP1/2, shown here to play an important role early in infection, possibly at the stage of nuclear capsid binding, contains a potent nuclear localization sequence (1). One can imagine importin-β recognizing and binding to incoming capsids via VP1/2's nuclear localization sequence or another region on the capsid and thus carrying the capsid cargo to the nucleus. Further, Nup358 has recently been shown to play an important role in importin α/β-dependent nuclear import (24). Once at the nucleus, capsid-bound importin-β could interact with Nup358 to anchor capsids to the NPC. Regardless of the involvement of other cellular factors, Nup358 appears to play an essential role in nuclear capsid binding.

ACKNOWLEDGMENTS

We thank the following generous contributors of reagents: Bryce Paschal, Timothy P. Bender, Günter Blobel and Elias Coutavas, Ari Helenius, and Frank Jenkins. We also thank Dean Kedes, Laura Adang, and Rebecca Mingo for many useful discussions of experimental results and Laura Adang, Fred Homa, and Lucy Pemberton for critical review of the manuscript.

This work was supported by NRSA fellowship 1 F31 NS055455-01A1 and NIH award AI041644.

REFERENCES

1. **Abaitua, F., and P. O'Hare.** 2008. Identification of a highly conserved, functional nuclear localization signal within the N-terminal region of herpes simplex virus type 1 VP1-2 tegument protein. J. Virol. **82:**5234–5244.
2. **Allen, T. D., J. M. Cronshaw, S. Bagley, E. Kiseleva, and M. W. Goldberg.** 2000. The nuclear pore complex: mediator of translocation between nucleus and cytoplasm. J. Cell Sci. **113:**1651–1659.
3. **Bastos, R., L. R. de Pouplana, M. Enarson, K. Bodoor, and B. Burke.** 1997. Nup84, A novel nucleoporin that is associated with CAN/Nup214 on the cytoplasmic face of the nuclear pore complex. J. Cell Biol. **137:**989–1000.
4. **Batterson, W., D. Furlong, and B. Roizman.** 1983. Molecular genetics of herpes simplex virus. VIII. Further characterization of a temperature-sensitive mutant defective in release of viral DNA and in other stages of the viral reproductive cycle. J. Virol. **45:**397–407.
5. **Beck, M., F. Förster, M. Ecke, J. M. Plitzko, F. Melchior, G. Gerisch, W. Baumeister, and O. Medalia.** 2004. Nuclear pore complex structure and dynamics revealed by cryoelectron tomography. Science **306:**1387–1390.
6. **Bernad, R., H. van der Velde, M. Fornerod, and H. Pickersgill.** 2004. Nup358/RanBP2 attaches to the nuclear pore complex via association with Nup88 and Nup214/CAN and plays a supporting role in CRM1-mediated nuclear protein export. Mol. Cell. Biol. **24:**2373–2384.
7. **Clarke, M. S., and P. L. McNeil.** 1992. Syringe loading introduces macromolecules into living mammalian cell cytosol. J. Cell Sci. **102:**533–541.
8. **Coller, K. E., J. I. H. Lee, A. Ueda, and G. A. Smith.** 2007. The capsid and tegument of the alphaherpesviruses are linked by an interaction between the UL25 and VP1/2 proteins. J. Virol. **81:**11790–11797.
9. **Cordes, V. C., S. Reidenbach, H. R. Rackwitz, and W. W. Franke.** 1997. Identification of protein p270/Tpr as a constitutive component of the nuclear pore complex-attached intranuclear filaments. J. Cell Biol. **136:**515–529.
10. **Cotten, M., and J. M. Weber.** 1995. The adenovirus protease is required for virus entry into host cells. Virology **213:**494–502.
11. **Cronshaw, J. M., A. N. Krutchinsky, W. Zhang, B. T. Chait, and M. J. Matunis.** 2002. Proteomic analysis of the mammalian nuclear pore complex. J. Cell Biol. **158:**915–927.
12. **Delphin, C., T. Guan, F. Melchior, and L. Gerace.** 1997. RanGTP targets p97 to RanBP2, a filamentous protein localized at the cytoplasmic periphery of the nuclear pore complex. Mol. Biol. Cell **8:**2379–2390.
13. **Desai, P., and S. Person.** 1998. Incorporation of the green fluorescent protein into the herpes simplex virus type 1 capsid. J. Virol. **72:**7563–7568.

14. **Dohner, K., A. Wolfstein, U. Prank, C. Echeverri, D. Dujardin, R. Vallee, and B. Sodeik.** 2002. Function of dynein and dynactin in herpes simplex virus capsid transport. Mol. Biol. Cell **13:**2795–2809.
15. **Fahrenkrog, B., J. Köser, and U. Aebi.** 2004. The nuclear pore complex: a jack of all trades? Trends Biochem. Sci. **29:**175–182.
16. **Gall, J. G.** 1967. Octagonal nuclear pores. J. Cell Biol. **32:**391–399.
17. **Goldberg, M. W., and T. D. Allen.** 1993. The nuclear pore complex: three-dimensional surface structure revealed by field emission, in-lens scanning electron microscopy, with underlying structure uncovered by proteolysis. J. Cell Sci. **106:**261–274.
18. **Granzow, H., F. Weiland, A. Jons, B. G. Klupp, A. Karger, and T. C. Mettenleiter.** 1997. Ultrastructural analysis of the replication cycle of pseudorabies virus in cell culture: a reassessment. J. Virol. **71:**2072–2082.
19. **Granzow, H., B. G. Klupp, and T. C. Mettenleiter.** 2005. Entry of pseudorabies virus: an immunogold-labeling study. J. Virol. **79:**3200–3205.
20. **Greber, U. F., M. Suomalainen, R. P. Stidwill, K. Boucke, M. W. Ebersold, and A. Helenius.** 1997. The role of the nuclear pore complex in adenovirus DNA entry. EMBO J. **16:**5998–6007.
21. **Greber, U. F., P. Webster, J. Weber, and A. Helenius.** 1996. The role of the adenovirus protease on virus entry into cells. EMBO J. **15:**1766–1777.
22. **Greber, U. F., M. Willetts, P. Webster, and A. Helenius.** 1993. Stepwise dismantling of adenovirus 2 during entry into cells. Cell **75:**477–486.
23. **Hase, M. E., and V. C. Cordes.** 2003. Direct interaction with Nup153 mediates binding of Tpr to the periphery of the nuclear pore complex. Mol. Biol. Cell **14:**1923–1940.
24. **Hutten, S., A. Flotho, F. Melchior, and R. H. Kehlenbach.** 2008. The Nup358-RanGAP complex is required for efficient importin α/β-dependent nuclear import. Mol. Biol. Cell **19:**2300–2310.
25. **Hutten, S., and R. H. Kehlenbach.** 2006. Nup214 is required for CRM1-dependent nuclear protein export in vivo. Mol. Cell. Biol. **26:**6772–6785.
26. **Jovasevic, V., L. Liang, and B. Roizman.** 2008. Proteolytic cleavage of VP1-2 is required for release of herpes simplex virus 1 DNA into the nucleus. J. Virol. **82:**3311–3319.
27. **Knipe, D. M., W. Batterson, C. Nosal, B. Roizman, and A. Buchan.** 1981. Molecular genetics of herpes simplex virus VI. Characterization of a temperature-sensitive mutant defective in the expression of all early viral gene products. J. Virol. **38:**539–547.
28. **Kraemer, D., R. W. Wozniak, G. Blobel, and A. Radu.** 1994. The human CAN protein, a putative oncogene product associated with myeloid leukemogenesis, is a nuclear pore complex protein that faces the cytoplasm. Proc. Natl. Acad. Sci. USA **91:**1519–1523.
29. **Leo, O., M. Foo, D. H. Sachs, L. E. Samelson, and J. A. Bluestone.** 1987. Identification of a monoclonal antibody specific for a murine T3 polypeptide. Proc. Natl. Acad. Sci. USA **84:**1374–1378.
30. **Lim, R., U. Aebi, and B. Fahrenkrog.** 2008. Towards reconciling structure and function in the nuclear pore complex. Histochem. Cell Biol. **129:**105–116.
31. **Lim, R. Y. H., K. S. Ullman, and B. Fahrenkrog.** 2008. Biology and biophysics of the nuclear pore complex and its components, p. 299–342. *In* W. J. Kwang (ed.), International review of cell and molecular biology. Academic Press, New York, NY.
32. **Luxton, G. W. G., S. Haverlock, K. E. Coller, S. E. Antinone, A. Pincetic, and G. A. Smith.** 2005. From the cover: targeting of herpesvirus capsid transport in axons is coupled to association with specific sets of tegument proteins. Proc. Natl. Acad. Sci. **102:**5832–5837.
33. **Maurer, U. E., B. Sodeik, and K. Grünewald.** 2008. Native 3D intermediates of membrane fusion in herpes simplex virus 1 entry. Proc. Natl. Acad. Sci. **105:**10559–10564.
34. **Newcomb, W. W., F. L. Homa, D. R. Thomsen, Z. Ye, and J. C. Brown.** 1994. Cell-free assembly of the herpes simplex virus capsid. J. Virol. **68:**6059–6063.
35. **Newcomb, W. W., F. P. Booy, and J. C. Brown.** 2007. Uncoating the herpes simplex virus genome. J. Mol. Biol. **370:**633–642.
36. **Newcomb, W. W., F. L. Homa, and J. C. Brown.** 2006. Herpes simplex virus capsid structure: DNA packaging protein UL25 is Located On the external surface of the capsid near the vertices. J. Virol. **80:**6286–6294.
37. **Newcomb, W. W., B. L. Trus, N. Cheng, A. C. Steven, A. K. Sheaffer, D. J. Tenney, S. K. Weller, and J. C. Brown.** 2000. Isolation of herpes simplex virus procapsids from cells infected with a protease-deficient mutant virus. J. Virol. **74:**1663–1673.
38. **Ojala, P. M., B. Sodeik, M. W. Ebersold, U. Kutay, and A. Helenius.** 2000. Herpes simplex virus type 1 entry into host cells: reconstitution of capsid binding and uncoating at the nuclear pore complex in vitro. Mol. Cell. Biol. **20:**4922–4931.
39. **Pante, N., R. Bastos, I. McMorrow, B. Burke, and U. Aebi.** 1994. Interactions and three-dimensional localization of a group of nuclear pore complex proteins. J. Cell Biol. **126:**603–617.
40. **Reichelt, R., A. Holzenburg, E. L. Buhle, Jr., M. Jarnik, A. Engel, and U. Aebi.** 1990. Correlation between structure and mass distribution of the nuclear pore complex and of distinct pore complex components. J. Cell Biol. **110:**883–894.
41. **Saphire, A. C. S., T. Guan, E. C. Schirmer, G. R. Nemerow, and L. Gerace.** 2000. Nuclear import of adenovirus DNA in vitro involves the nuclear protein import pathway and hsc70. J. Biol. Chem. **275:**4298–4304.
42. **Shelton, L. S., A. G. Albright, W. T. Ruyechan, and F. J. Jenkins.** 1994. Retention of the herpes simplex virus type 1 (HSV-1) UL37 protein on single-stranded DNA columns requires the HSV-1 ICP8 protein. J. Virol. **68:**521–525.
43. **Sodeik, B., M. W. Ebersold, and A. Helenius.** 1997. Microtubule-mediated transport of incoming herpes simplex virus 1 capsids to the nucleus. J. Cell Biol. **136:**1007–1021.
44. **Suntharalingam, M., and S. R. Wente.** 2003. Peering through the pore: nuclear pore complex structure, assembly, and function. Dev. Cell **4:**775–789.
45. **Tognon, M., D. Furlong, A. J. Conley, and B. Roizman.** 1981. Molecular genetics of herpes simplex virus. V. Characterization of a mutant defective in ability to form plaques at low temperatures and in a viral fraction which prevents accumulation of coreless capsids at nuclear pores late in infection. J. Virol. **40:**870–880.
46. **Trotman, L. C., N. Mosberger, M. Fornerod, R. P. Stidwill, and U. F. Greber.** 2001. Import of adenovirus DNA involves the nuclear pore complex receptor CAN/Nup214 and histone H1. Nat. Cell Biol. **3:**1092–1100.
47. **Walther, T. C., H. S. Pickersgill, V. C. Cordes, M. W. Goldberg, T. D. Allen, I. W. Mattaj, and M. Fornerod.** 2002. The cytoplasmic filaments of the nuclear pore complex are dispensable for selective nuclear protein import. J. Cell Biol. **158:**63–77.
48. **Wolfstein, A., C. H. Nagel, K. Radtke, K. Dohner, V. J. Allan, and B. Sodeik.** 2006. The inner tegument promotes herpes simplex virus capsid motility along microtubules in vitro. Traffic **7:**227–237.
49. **Wu, J., M. J. Matunis, D. Kraemer, G. Blobel, and E. Coutavas.** 1995. Nup358, a cytoplasmically exposed nucleoporin with peptide repeats, Ran-GTP binding sites, zinc fingers, a cyclophilin A homologous domain, and a leucine-rich region. J. Biol. Chem. **270:**14209–14213.
50. **Yokoyama, N., N. Hayashi, T. Seki, N. Pante, T. Ohba, K. Nishii, K. Kuma, T. Hayashida, T. Miyata, U. Aebi, M. Fukui, and T. Nishimoto.** 1995. A giant nucleopore protein that binds Ran/TC4. Nature **376:**184–188.
51. **Zhou, Z. H., D. H. Chen, J. Jakana, F. J. Rixon, and W. Chiu.** 1999. Visualization of tegument-capsid interactions and DNA in intact herpes simplex virus type 1a virions. J. Virol. **73:**3210–3218.